

THERMAL CONDUCTION IN GALAXY-CLUSTER PLASMAS AND THE DIVERGENCE OF NEIGHBORING MAGNETIC FIELD LINES IN STRONG MAGNETOHYDRODYNAMIC TURBULENCE

BENJAMIN D. G. CHANDRAN
 benjamin-chandran@uiowa.edu

JASON L. MARON
 jason-maron@uiowa.edu

Center for Magnetic Reconnection Studies, Department of Physics & Astronomy, University of Iowa
 Draft version May 22, 2019

ABSTRACT

Galaxy clusters possess turbulent magnetic fields with a dominant scale length $l_B \sim 1 - 10$ kpc. In the static-magnetic-field approximation, the thermal conductivity κ_T for heat transport over distances $\gg l_B$ in clusters is $\sim \kappa_S l_B / L_S(\rho_e)$, where κ_S is the Spitzer thermal conductivity for a non-magnetized plasma, the length $L_S(r_0)$ is a characteristic distance that a pair of field lines separated by a distance $r_0 < l_B$ at one location must be followed before they separate by a distance l_B , and ρ_e is the electron gyroradius. We introduce an analytic Fokker-Planck model and a numerical Monte Carlo model of field-line separation in strong magnetohydrodynamic (MHD) turbulence to calculate $L_S(r_0)$. Like earlier models, these models predict that L_S asymptotes to a constant value of order l_B as $r_0/l_B \rightarrow 0$ and $l_d/l_B \rightarrow 0$ provided r_0 is not vastly smaller than l_d , where l_d is the dissipation scale. On the other hand, using direct numerical simulations of MHD turbulence we find that $(L_S/l_B) \simeq 1.8 + 1.3 \ln(l_B/r_0)$ in the small- (r_0/l_B) limit. We argue that our approximate Fokker-Planck and Monte-Carlo models, like earlier models, underestimate L_S because of intermittency. Our numerical results imply that $\kappa_T \sim \kappa_S/50$ for typical cluster parameters in the static-field approximation, a value that is too small for thermal conduction to balance radiative cooling.

Turbulent fluid motions enhance κ_T to some degree. We will address turbulent diffusion in a future paper. In this paper, we show that under the questionable assumption that turbulent resistivity completely reconnects field lines on the time scale l_B/u , where u is the rms turbulent velocity, the value of κ_T in cluster conditions is increased to $\sim \sqrt{\kappa_S u l_B}$, where κ_S and κ_T are expressed as diffusion coefficients. It is possible that interchange-like mixing of field lines by Alfvénic turbulence coupled with rapid single-electron motion enhances κ_T to a similar value, even if field lines aren't completely reconnected in a time l_B/u . However, turbulent reconnection and field-line mixing in a tangled magnetic field are not well understood, and further work is required before firm conclusions can be drawn about their effects on κ_T . We present numerical simulations of field-line separation in different types of MHD turbulence with different initial conditions in a companion paper.

1. INTRODUCTION

In the cooling-flow (CF) model of intracluster plasma, radiative cooling via x-ray emission causes plasma to flow towards a cluster's center and cool to sub-x-ray temperatures, presumably ending up as either stars, smaller compact objects, and/or cold gas. Aside from the gravitational work done on inflowing plasma, heating of intracluster plasma is neglected in the model, and mass accretion rates \dot{M} are as high as $10^3 M_\odot \text{ yr}^{-1}$ for some clusters (Fabian 1994). A longstanding problem for the CF model has been the difficulty in accounting for all the accreted mass. For example, the observed rates of massive star formation are a factor of 10-100 less than expected if the cooling plasma predicted by the model ends up forming stars with a normal IMF (Crawford et al 1999, Fabian 2002). In addition, recent x-ray observations find no evidence of plasma cooling to temperatures below 1-2 keV (Peterson et al 2001, Tamura et al 2001). These difficulties suggest that some form of heating approximately balances radiative cooling, thereby dramatically reducing \dot{M} relative to CF estimates. A number of heating mechanisms have been considered, such as galaxy motions (Bregman & David 1989), supernovae (Bregman & David 1989), cosmic-rays (Bohringer & Morfill 1988, Tucker & Rosner 1983), active galactic nuclei (Pedlar et al 1990, Tabor & Binney 1993, Binney & Tabor 1995, Ciotti & Ostriker 2001, Churazov et al 2002), and thermal conduction, which can trans-

port heat from the hot outer regions of a cluster into the relatively cooler core (Narayan & Medvedev 2001, Gruzinov 2002, Voigt et al 2002, Zakamska & Narayan 2003). For thermal conduction to approximately balance cooling, the thermal conductivity κ_T must be a significant fraction of the Spitzer value for a non-magnetized plasma, κ_S , and in some clusters even greater than κ_S (Fabian 2002, Zakamska & Narayan 2002).

Galaxy clusters are filled with tangled magnetic fields with a dominant length scale $l_B \sim 1 - 10$ kpc (Kronberg 1994, Taylor et al 2001, 2002) that is much less than the size of a cluster core, $R_c \sim 100$ kpc. Optical-line-emitting gas in clusters is observed to be in turbulent motion (Fabian 1994), and the hot plasma is presumably turbulent as well. The effects of turbulent magnetic fields and velocities on κ_T are the subject of this paper, and have been investigated by a number of authors (e.g., Tribble 1989, Tao 1995, Chandran & Cowley 1998, Chandran et al 1999, Narayan & Medvedev 2001, Malyshevskii & Kulsrud 2001, Gruzinov 2002).

Transport in the presence of strong turbulence is a difficult and unsolved problem. It is likely that the thermal conductivity for a particle species scales like the test-particle diffusion coefficient for that particle species (Rechester & Rosenbluth 1978, Krommes, Oberman, & Kleva 1983): since the collisional transfer of energy between particles occurs locally in space, diffusion of heat accompanies the diffusion of heat-carrying particles. We thus estimate κ_T in clusters from the

relation

$$\frac{\kappa_T}{\kappa_S} \simeq \frac{D}{D_0}, \quad (1)$$

where D is the diffusion coefficient of thermal electrons and D_0 is the thermal-electron diffusion coefficient in a non-magnetized plasma.^{1 2 3}

Since thermal electrons in clusters move much faster than the $\mathbf{E} \times \mathbf{B}$ velocity of field lines, a reasonable first approximation for D is obtained by treating the magnetic field as static. In a collisional plasma, particle diffusion over distances $\gg l_B$ in a static field depends critically on the rate of separation of neighboring magnetic field lines (Rechester & Rosenbluth 1978, Chandran & Cowley 1998). If two field lines within a snapshot of strong magnetohydrodynamic (MHD) turbulence are at some location separated by a distance $r_0 \ll l_B$, they will separate by a distance l_B after some distance z along the magnetic field. The length $L_S(r_0)$ is a characteristic value of z defined in section 2. In the static-magnetic field approximation, the thermal conductivity κ_T in galaxy clusters over distances $\gg l_B$ satisfies

$$\kappa_T \simeq \frac{\kappa_S l_B}{L_S(\rho_e)}, \quad (2)$$

where ρ_e is the electron gyroradius. Equation (2) makes use of the fact that electron motion along the magnetic field is relatively unimpeded by magnetic mirrors and whistler waves excited by the heat flux because the Coulomb mean free path is short compared to both L_B and the temperature-gradient length scale (see section 3). The factor $l_B/L_S(\rho_e)$ in equation (2) measures the reduction in κ_T associated with tangled field lines, which increase the distance electrons must travel in going from hotter regions to colder regions.

Three previous studies (Jokipii 1973, Skilling, McIvor, & Holmes 1974, Narayan & Medvedev 2001) calculated $L_S(r_0)$ assuming a turbulent power spectrum of magnetic fluctuations on scales ranging from l_B to a much smaller dissipation scale l_d , which is approximately the proton gyroradius ρ_i in galaxy clusters (Quataert 1998). Using different definitions of L_S , each study found that $L_S(r_0) \simeq l_B$ in the small- (r_0/l_B) and small- l_d/l_B limits provided r_0 was not vastly smaller than l_d . Jokipii (1973) assumed an isotropic turbulent magnetic field and employed a stochastic model of field-line separation, which he solved using a Monte Carlo numerical method. Skilling et al (1974) assumed isotropic turbulence and introduced an approximate equation of the form $d\langle r \rangle/dz = F(\langle r \rangle)$ for the average separation r of a pair of field lines, with the function F estimated from the power spectrum of the turbulence. Narayan & Medvedev (2001) introduced a similar equation for the evolution of the mean square separation, $d\langle r^2 \rangle/dl = G(\langle r^2 \rangle)$, and estimated G using the anisotropic Goldreich-Sridhar (GS) (1995) model of MHD turbulence.

In this paper, we calculate L_S using three different methods. First, we consider an approximate model in which the separation r of a pair of field lines evolves stochastically and is de-

scribed by the Fokker-Planck equation

$$\frac{\partial P}{\partial l} = -\frac{\partial}{\partial y} \left[\left(\frac{\langle \Delta y \rangle}{\Delta l} \right) P \right] + \frac{\partial^2}{\partial y^2} \left[\left(\frac{\langle (\Delta y)^2 \rangle}{2\Delta l} \right) P \right], \quad (3)$$

where $y = \ln(r/l_B)$, l is distance traveled along the field in units of l_B , Δy is the increment to y after a field-line pair is followed a distance Δl along the field, $\langle \dots \rangle$ is an average over a large number of field-line pairs, and $P(y, l)dy$ is the probability that $\ln(r/l_B)$ is in the interval $(y, y+dy)$ after a distance l along the field. Our model is similar to Jokipii's (1973), although we determine the functional form of $\langle \Delta y \rangle/\Delta l$ and $\langle (\Delta y)^2 \rangle/\Delta l$ using the anisotropic GS model of MHD turbulence, and we solve the Fokker Planck equation analytically, which allows us to determine the functional dependence of L_S on turbulence parameters. Like the earlier studies, our calculation yields $L_S(r_0) \sim l_B$ in the small- r_0/l_B and small- l_d/l_B limits provided r_0 is not vastly smaller than l_d . Even if $\langle \Delta y \rangle/\Delta l = 0$, so that instantaneously a field line pair is equally likely to diverge or converge, we find that $L_S \sim l_B$ in the small- l_d/l_B and small- r_0/l_B limits [assuming $\langle (\Delta y)^2 \rangle/\Delta l$ given by the GS model], provided r_0 is not vastly smaller than l_d . Thus, the stochastic nature of field-line separation does not dramatically enhance L_S relative to the value predicted by a non-stochastic model with $\langle (\Delta y)^2 \rangle/\Delta l = 0$, and the analytic model can not explain the logarithmic dependence of L_S on r_0 for $l_d < r_0 < l_B$ that we find in our direct numerical simulations, as discussed below.

Our second method for calculating $L_S(r_0)$ uses an approximate Monte-Carlo model of field line separation in which each random step Δy is of order unity (the Fokker-Planck equation assumes infinitesimal Markovian steps). We solve this model numerically and obtain results similar to those of the Fokker-Planck model.

Our third method for calculating $L_S(r_0)$ involves tracking field-line trajectories in direct numerical simulations of MHD turbulence. For MHD turbulence without a mean magnetic field, we find that

$$\frac{L_S}{l_B} = 1.8 + 1.3 \ln \left(\frac{l_B}{r_0} \right) \quad (4)$$

in the small- (r_0/l_B) limit for $r_0 > l_d$, with a similar scaling for $r_0 < l_d$. We also find a logarithmic scaling for L_S in simulations of MHD turbulence with a mean magnetic field. We calculate L_S by tracking field lines in numerically generated random-phase magnetic fields with the same Fourier amplitudes as the turbulent fields in our direct numerical simulations. The results of the random-phase calculations are consistent with the Fokker-Planck and Monte-Carlo results: L_S appears to asymptote to a constant value of a few times l_B in the small- r_0/l_B and small- l_d/l_B limits provided r_0 is not vastly smaller than l_d . The key difference between the direct numerical simulations and random-phase fields is intermittency. In the direct numerical simulations, the magnetic shear is concentrated into sheet-like structures elongated along the magnetic field that fill a small fraction of the volume, while a large fraction of the volume is filled with comparatively weak magnetic shear. A field-line pair can thus be followed for a long distance in the direct numerical

¹ Electrons make the dominant contribution to κ_T because they diffuse more rapidly than ions.

² In a steady state, an electric field is set up to maintain quasi-neutrality. This electric field reduces κ_T by a factor of ~ 0.4 in a non-magnetized plasma (Spitzer 1962). We do not consider the effects of turbulence on this reduction factor.

³ There is some ambiguity in the right-hand side of equation (1). We take D and D_0 to be diffusion coefficients for particles of a specified energy as opposed to diffusion coefficients of a particle that diffuses in energy as well as space. Thus, D/D_0 may scale differently for electrons of energies, e.g., $k_B T$ and $2k_B T$. In the static-field approximation this is not an issue since D/D_0 is the same for all energies of interest for cluster parameters. However, when we estimate the effects of turbulent resistivity, we pick a representative energy at which to evaluate D/D_0 as discussed in section 7.

simulations before it enters a high-magnetic-shear region. This limits the ability of small-scale magnetic structures to separate the majority of closely spaced field-line pairs. Our numerical results imply that $L_S \sim 46l_B$ for galaxy-cluster plasmas, and thus that $\kappa_T \sim \kappa_S/46$ for conduction over distances $\gg l_B$ in the static-field approximation, a value that is too small for thermal conduction to balance radiative cooling.

Field evolution and turbulent fluid motions enhance κ_T to some degree. We will address turbulent diffusion in a future paper. In this paper, we show that under the questionable assumption that turbulent resistivity completely reconnects field lines on the time scale l_B/u , where u is the rms turbulent velocity, the value of κ_T in cluster conditions is increased to a value $\sim \sqrt{\kappa_S u l_B}$. It is possible that interchange-like mixing of field lines by Alfvénic turbulence coupled with rapid single-electron motion enhances κ_T to a similar value, even if field lines aren't completely reconnected in a time l_B/u . Additional study of turbulent resistivity and field-line mixing is needed before firm conclusions can be drawn about their effects on κ_T .

The remainder of this paper is organized as follows. In section 2 we review the phenomenology of thermal conduction in static tangled magnetic fields. In section 3, we discuss the effects of magnetic mirrors and microturbulence on electron diffusion along field lines. We present our Fokker-Planck and Monte Carlo models of field-line separation in section 4. We compare these approximate theoretical models with results from direct numerical simulations in section 5, and give a numerical example illustrating the results of the static-field approximation in section 6. We estimate the effects of turbulent resistivity on κ_T and discuss field-line mixing in section 7 and summarize our conclusions in section 8. We present numerical simulations of different types of MHD turbulence with different initial conditions in a companion paper (Maron, Chandran, & Blackman 2003).

Table 1 defines some frequently used notation.

2. THE PHENOMENOLOGY OF THERMAL CONDUCTION IN A STATIC TANGLED MAGNETIC FIELD

We assume that the magnetic fluctuations possess an inertial range extending from an outer scale l_B to a much smaller inner scale l_d with the magnetic energy dominated by scales $\sim l_B$. Except where specified, the discussion focuses on the case relevant for clusters in which there is no mean magnetic field pervading the plasma.

A tangled magnetic field line is essentially a random-walk path through space. If a particle is tied to a single field line and travels a distance $l > l_B$ along the static magnetic field, it takes l/l_B random-walk steps of length l_B , resulting in a mean-square three-dimensional displacement of

$$\langle(\Delta x)^2\rangle = \alpha l_B l, \quad (5)$$

where α is a constant of order unity (values of α for the numerical simulations used in this paper are listed in table 2). When there is a mean field \mathbf{B}_0 comparable to the rms field, $\langle(\Delta x)^2\rangle$ in equation (5) is interpreted as the mean-square displacement perpendicular to \mathbf{B}_0 . If the particle's motion along the field is diffusive with diffusion coefficient D_{\parallel} , then

$$l \sim \sqrt{D_{\parallel} t}, \quad (6)$$

and (Rechester & Rosenbluth 1978, Krommes et al 1983)

$$\langle(\Delta x)^2\rangle \propto t^{1/2}, \quad (7)$$

indicating subdiffusion: $D \equiv \lim_{t \rightarrow \infty} \langle(\Delta x)^2\rangle/t \rightarrow 0$. This process is called double diffusion: the particle diffuses along the field line, and the field line itself is a random-walk path through space.

The vanishing of D for a particle tied to a single field line can be understood by considering a particle starting out at point P in figure 1. If this particle moves one Coulomb mean free path λ along its field line F_1 towards point Q and then randomizes its velocity due to collisions, it has a $\sim 50\%$ chance of changing its direction of motion along the magnetic field and returning to its initial point P. In contrast, in a Markovian three dimensional random walk, the second step is uncorrelated from the first and there is a vanishing probability that a particle will return to its initial location. In a cluster, $\rho_e/l_B \simeq 10^{-15}$, and thus it is tempting to assume that electrons are tied to field lines. The importance of equation (7) is that any study that assumes that electrons are perfectly tied to field lines will conclude that $\kappa_T = D = 0$.

Of course, an electron is not tied to a single field line. As pointed out by Rechester & Rosenbluth (1978), small cross-field motions enhanced by the divergence of neighboring field lines leads to a non-zero D . This can be seen with the aid of figure 1. Suppose an electron starts out at point P on field line F_1 traveling towards point Q. After moving a short distance, field gradients and collisions cause the particle to take a step of length $\sim \rho_e$ across the magnetic field, from F_1 to a new field line F_2 . Although the electron continuously drifts across the field to new field lines, let us assume for the moment that it remains attached to F_2 . As the electron follows F_2 , F_2 diverges from F_1 . Let z be the distance that F_2 must be followed before F_2 separates from F_1 by a distance l_B . (Because the electron continuously drifts across the field, it typically separates from F_1 after traveling a distance somewhat less than z along the field; this effect, however, is ignored in this paper.) After the electron moves a distance z along F_2 , its subsequent motion is not correlated with F_1 . The electron proceeds to point R, and then its collisional random walk along the magnetic field changes direction, bringing it back towards point Q. Instead of following F_2 back to point Q, however, the electron drifts across the field and ends up on a new field line F_3 . After following F_3 for a distance $\sim z$, the electron separates from F_2 by a distance $\sim l_B$ and proceeds to point S.

In this example, the electron's small cross-field motions and the divergence of neighboring field lines allow the electron to escape from its initial field line and undergo a Markovian random walk in three dimensions. The fundamental random walk step is a displacement of length mz along the magnetic field, where m is some constant of order unity, perhaps 2 or 3. From equation (5), when $mz \gg l_B$, a single random step corresponds to a 3D displacement of

$$\langle(\Delta x)^2\rangle \sim \alpha m z l_B. \quad (8)$$

When $mz \gg \lambda$, where λ is the Coulomb mean free path, a single step takes a time

$$\Delta t \sim \frac{m^2 z^2}{D_{\parallel}}. \quad (9)$$

When mz is only moderately greater than l_B or λ , equations (8) and (9) remain approximately valid. During successive random steps, a particle will find itself in regions of differing magnetic shear, and thus z will vary. The diffusion coefficient is given by

$D = \langle (\Delta x)^2 \rangle / \langle \Delta t \rangle$ where $\langle \dots \rangle$ is an average over a large number of steps (Chandrasekhar 1943). Ignoring factors of order unity we obtain⁴

$$D \sim \frac{D_{\parallel} l_B}{L_S}, \quad (10)$$

with

$$L_S = \frac{\langle z^2 \rangle}{\langle z \rangle}. \quad (11)$$

Elsewhere, we use the notation $L_S(r_0)$, where r_0 is the initial separation of a pair of field lines. The notation L_S is shorthand for $L_S(\rho_e)$. If there is a mean magnetic field comparable to the fluctuating field, equation (10) is recovered provided D is replaced by D_{\perp} , the coefficient of diffusion perpendicular to the mean field. We note that taking $L_S = \langle z \rangle$ leads to similar results since $\langle z \rangle \sim \langle z^2 \rangle / \langle z \rangle$ in our direct numerical simulations and Fokker-Planck and Monte Carlo calculations. In clusters $D_{\parallel} \sim D_0$ as discussed in section 3, where D_0 is the electron diffusion coefficient in a non-magnetized plasma. As a result, equations (1) and (11) give

$$\kappa_T = \frac{\kappa_S l_B}{L_S}. \quad (12)$$

3. ELECTRON DIFFUSION ALONG THE MAGNETIC FIELD

For mono-energetic electrons subject to a fixed Coulomb pitch-angle scattering frequency, the diffusion coefficient $D_{\parallel,0}$ for motion along a uniform magnetic field is equal to the three-dimensional diffusion coefficient D_0 for motion in a non-magnetized plasma. Two mechanisms for suppressing D_{\parallel} relative to $D_{\parallel,0}$ have been discussed in the literature: magnetic mirrors and wave pitch angle scattering. Magnetic mirrors associated with a cluster's turbulent magnetic field significantly reduce D_{\parallel} only when $\lambda \gtrsim l_B$, where λ is the Coulomb mean free path of thermal electrons (Chandran & Cowley 1998, Mal'ushkin & Kulsrud 2001). In cluster cores, however, λ is significantly less than l_B , and thus mirrors have only a small effect. [For Hydra A and 3C295, $\lambda \sim 1$ kpc at 100 kpc from cluster center, and $\lambda = 0.02 - 0.05$ kpc at 10 kpc from cluster center (Narayan & Medvedev 2001).] When the Knudsen number $N_K \equiv \lambda/L_{T,\parallel}$ approaches 1, where $L_{T,\parallel} = T/|\hat{\mathbf{b}} \cdot \nabla T|$ and $\hat{\mathbf{b}}$ is a unit vector pointing along the magnetic field, the heat flux becomes large and excites whistler waves that enhance the pitch-angle scattering of electrons and reduce D_{\parallel} (Pistinner & Eichler 1998)⁵. However, for heat conduction into a cluster core, $|\nabla T| \sim T/R_c$ with $R_c \sim 100$ kpc, and $N_K \ll 1$. Thus, wave pitch-angle scattering has only a small effect, and

$$D_{\parallel} \sim D_0. \quad (13)$$

We note that the chaotic trajectories of field lines cause $L_{T,\parallel}$ to be larger than $T/|\nabla T|$.

4. FOKKER-PLANCK AND MONTE CARLO MODELS OF FIELD-LINE SEPARATION IN STRONG MHD TURBULENCE

We adopt the Goldreich & Sridhar (1995) (hereafter GS) model of strong anisotropic MHD turbulence, which is supported by direct numerical simulations (Cho & Vishniac 2000,

Maron & Goldreich 2001, Cho & Lazarian 2003). We assume that the fluctuating field is equal to or greater than any mean field in the system. The separation of neighboring magnetic field lines in strong MHD turbulence is dominated by shear Alfvén modes. On scales smaller than l_B , an Alfvén-mode eddy is elongated along the direction of the average of the magnetic field within the volume of the eddy, denoted $\mathbf{B}_{\text{local}}$, with (Goldreich & Sridhar 1995, Cho & Vishniac 2000, Maron & Goldreich 2001, Lithwick & Goldreich 2001)

$$B_{\lambda_{\perp}} \sim B_{\text{local}} \left(\frac{\lambda_{\perp}}{l_B} \right)^{1/3}, \quad (14)$$

and

$$\lambda_{\parallel} \sim \lambda_{\perp}^{2/3} l_B^{1/3}, \quad (15)$$

where $B_{\lambda_{\perp}}$ is the rms magnetic fluctuation of an Alfvén-mode eddy of width λ_{\perp} measured across $\mathbf{B}_{\text{local}}$ and length λ_{\parallel} measured along $\mathbf{B}_{\text{local}}$. In fully ionized plasmas, the dissipation scale l_d for Alfvén modes is set by collisionless effects, and is comparable to the proton gyroradius ρ_i (Quataert 1998). The magnetic-field perturbation of an Alfvén mode is perpendicular to $\mathbf{B}_{\text{local}}$. Equations (14) and (15) thus imply that when two field lines separated by a distance r are followed for a distance $r^{2/3} l_B^{1/3}$, r either increases or decreases by a factor of order unity assuming $l_d < r < l_B$ (Narayan & Medvedev 2001, Maron & Goldreich 2001, Lithwick & Goldreich 2001). If $r < l_d$, the separation or convergence of the field lines is dominated by the eddies of width l_d , and r increases or decreases by a factor of order unity when the field lines are followed a distance $l_d^{2/3} l_B^{1/3}$ (Narayan & Medvedev 2001). We define

$$\Delta l = \begin{cases} (r/l_B)^{2/3} & \text{if } l_d < r < l_B \\ (l_d/l_B)^{2/3} & \text{if } r < l_d \end{cases}, \quad (16)$$

$$y = \ln(r/l_B), \quad (17)$$

Δy to be the increment to y when the field lines are followed a distance Δl ,

$$a = \langle \Delta y \rangle, \quad (18)$$

with a taken to be nonnegative, and

$$b = \langle (\Delta y)^2 \rangle / 2, \quad (19)$$

where a and b are of order unity.

To obtain Monte Carlo and analytic solutions for L_S , we make several approximations. The changes in r over a distance $r^{2/3} l_B^{1/3}$ along the field associated with eddies of width much smaller or larger than r (or l_d if $r < l_d$) are small compared to the changes arising from eddies of width r (or l_d if $r < l_d$) and are neglected. We also take a and b to be independent of l and y , and consecutive values of Δy to be uncorrelated. To obtain an approximate analytic solution for L_S , we make the further approximation of describing the stochastic variation of y with the Fokker-Planck equation

$$\frac{\partial P}{\partial l} = -\frac{\partial}{\partial y} \left[\left(\frac{\langle \Delta y \rangle}{\Delta l} \right) P \right] + \frac{\partial^2}{\partial y^2} \left[\left(\frac{\langle (\Delta y)^2 \rangle}{2 \Delta l} \right) P \right], \quad (20)$$

where $P(y', l) dy$ is the probability that y is in the interval $(y', y' + dy)$, and l is distance travelled along the magnetic field

⁴ In applying equation (8) first and then averaging z and z^2 , we are averaging separately over the wandering of a single field line through space and the separation of neighboring field lines. This is justified to some extent since the former is dominated by the value of \mathbf{B} at the outer scale and the latter depends on the magnetic shear throughout the inertial range. Although some error is introduced by averaging separately, equations (10) and (11) are sufficient for estimating κ_T .

⁵ The formula in Pistinner & Eichler's (1998) paper is $\kappa_T/\kappa_S \sim 1/[1 + 250\beta_e(\lambda/L_{T,\parallel})]$, but the factor of 250 should be corrected to a factor of 10 (Pistinner, private communication)

in units of l_B . The additional approximation in introducing equation (20) is associated with y changing by order unity during a single random step [equation (20) assumes infinitesimal steps].

We now solve equation (20) to obtain an analytic solution for L_S . Substituting equations (16), (18), and (19) into equation (20) yields

$$\frac{\partial P}{\partial l} = -\frac{\partial \Gamma}{\partial y}, \quad (21)$$

where

$$\Gamma = \begin{cases} ae^{-2y/3}P - \frac{\partial}{\partial y}(be^{-2y/3}P) & \text{if } y_d < y < 0 \\ ae^{-2y_d/3}P - be^{-2y_d/3}\frac{\partial P}{\partial y} & \text{if } y < y_d \end{cases}, \quad (22)$$

is the probability flux, and

$$y_d = \ln\left(\frac{d}{l_B}\right), \quad (23)$$

which is the value of y at the dissipation scale. We solve equation (21) with initial condition $P(y) = \delta(y - y_0)$ at $l = 0$ and boundary conditions $P = 0$ at $y = 0$, $P \rightarrow 0$ as $y \rightarrow -\infty$, and P and Γ continuous at $y = y_d$. For electron thermal conduction in galaxy clusters, the quantity of interest is L_S when the initial separation r_0 is the electron gyroradius, and thus we take $y_0 < y_d$. The boundary condition $P = 0$ at $y = 0$ means that $\Gamma(l, y = 0)dl$ gives the probability that a field-line pair separates to a distance l_B for the first time after a distance between l and $l + dl$ along the field.

We proceed by making the substitution

$$P = x^m f, \quad (24)$$

with

$$x = e^{y/3} \quad (25)$$

and

$$m = 2 + 3a/2b. \quad (26)$$

We then take the Laplace transform of equation (21), with the Laplace transform of f defined by

$$\bar{f}(s) = \int_0^\infty f(l)e^{-sl}dl. \quad (27)$$

For $x_d < x < 1$, where $x_d = e^{y_d/3}$ is the value of x at the dissipation scale,

$$\frac{\partial^2 \bar{f}}{\partial x^2} + \frac{1}{x} \frac{\partial \bar{f}}{\partial x} - \left(\frac{v^2}{x^2} + \frac{9s}{b}\right) \bar{f} = 0, \quad (28)$$

with

$$v = \frac{3a}{2b}. \quad (29)$$

Since $f(1) = 0$,

$$\bar{f} = c_1 [I_v(\psi x) K_v(\psi) - K_v(\psi x) I_v(\psi)], \quad (30)$$

where I_v and K_v are modified Bessel's functions,

$$\psi = 3\sqrt{\frac{s}{b}}, \quad (31)$$

and c_1 is a constant to be determined by applying the boundary conditions at x_d after the solution for \bar{f} for $x < x_d$ has been obtained.

For $x < x_d$,

$$\frac{\partial^2 \bar{f}}{\partial x^2} + \frac{1}{x} \frac{\partial \bar{f}}{\partial x} + \frac{(4 - v^2 - \chi)\bar{f}}{x^2} = -\frac{3x_d^2 x_0^{-m-1} \delta(x - x_0)}{b}, \quad (32)$$

where

$$\chi = \frac{9x_d^2 s}{b} \quad (33)$$

and

$$x_0 = e^{y_0/3}. \quad (34)$$

For $x < x_0$,

$$\bar{f} = c_2 x^{-2+\sqrt{v^2+\chi}} + c_3 x^{-2-\sqrt{v^2+\chi}}. \quad (35)$$

For $x_0 < x < x_d$,

$$\bar{f} = c_4 x^{-2+\sqrt{v^2+\chi}} + c_5 x^{-2-\sqrt{v^2+\chi}}. \quad (36)$$

For $\text{Re}(s) \geq 0$, the boundary condition at $y = -\infty$ implies that $c_3 = 0$. Integrating equation (32) from $x_0 - \varepsilon$ to $x_0 + \varepsilon$ yields the jump condition for $\partial \bar{f} / \partial x$ at $x = x_0$. After applying this jump condition and the continuity of f and Γ at $x = x_d$, we find that

$$c_1 = \frac{3x_0^{-v+\sqrt{v^2+\chi}} x_d^{-\sqrt{v^2+\chi}}}{b(hT - \psi x_d U)}, \quad (37)$$

where

$$T = I_v(\psi x_d) K_v(\psi) - K_v(\psi x_d) I_v(\psi), \quad (38)$$

and

$$U = I'_v(\psi x_d) K_v(\psi) - K'_v(\psi x_d) I_v(\psi). \quad (39)$$

Since $I'_v(\psi) K_v(\psi) - K'_v(\psi) I_v(\psi) = 1/\psi$, we find that

$$\bar{\Gamma}(x = 1) = -\frac{bc_1}{3}. \quad (40)$$

Since

$$\langle l^n \rangle = \int_0^\infty dl l^n \Gamma \Big|_{x=1} = \left(\frac{\partial}{\partial s} \right)^n \bar{\Gamma} \Big|_{x=1, s=0}, \quad (41)$$

where n is a non-negative integer, we have

$$\langle l^n \rangle = -\frac{b}{3} \frac{\partial^n c_1}{\partial s^n} \Big|_{s=0}. \quad (42)$$

Thus,

$$\langle l \rangle = \frac{9}{b} \left[\frac{1}{4(v+1)} + \frac{x_d^2}{2v} \ln\left(\frac{x_d}{x_0}\right) - \frac{x_d^2}{4v^2} \left(v - 1 + \frac{x_d^{2v}}{v+1} \right) \right]. \quad (43)$$

For $x_d \ll 1$ and $x_d^2 \ln(x_d/x_0) \ll 1$, equation (43) gives

$$\langle l \rangle = \frac{9}{2(2b+3a)}. \quad (44)$$

The full equation for $\langle l^2 \rangle$ is very long and will not be quoted here. However, for $x_d \ll 1$ and $x_d^2 \ln(x_d/x_0) \ll 1$, we find that

$$\langle l^2 \rangle = \frac{81(3a+6b)}{4(3a+2b)^2(3a+4b)}, \quad (45)$$

with $L_S/l_B = \langle l^2 \rangle / \langle l \rangle$ given by

$$\frac{L_S}{l_B} = \frac{9(3a+6b)}{2(3a+2b)(3a+4b)}. \quad (46)$$

We now check the analytic results with a Monte Carlo solution of equation (20) with initial conditions $P(y, l = 0) = \delta(y - y_0)$, and with $y_0 = -10$ and $y_d = -8$. The Monte Carlo solution consists of iteratively incrementing a pair of numbers (l, y) . During each step, we increase l by an amount $\delta l = e^{2y/3} \phi$ (or $\delta l = e^{2y_d/3} \phi$ if $y < y_d$) and increase y by an amount $\delta y = a\phi \pm k$, where the \pm sign is determined randomly with equal chance for either sign, and ϕ is a constant. As $\phi \rightarrow 0$,

each step becomes infinitesimal as is assumed in the Fokker-Planck equation. The value of k is chosen so that $\langle(\delta y)^2\rangle = 2b\phi$ (i.e., $k = \sqrt{2b\phi - a^2\phi^2}$). We stop incrementing l and y once y reaches 0, and record the value of l at the final step. We repeat this for 2000 ordered pairs to obtain $\langle l \rangle$ and $\langle l^2 \rangle$. The results of this procedure with $\phi = 10^{-4}$ and $a = 0.3$ for various values of b are shown in figure 2, along with the analytic results of equations (44) and (45). We also plot Monte Carlo results with $\phi = 1$, which provide a measure of the error associated with using a Fokker-Planck equation to describe the discrete stochastic process described by equations (16), (18), and (19).

5. DIRECT NUMERICAL SIMULATIONS

In this section, we report calculations of field-line separation in two direct numerical simulations of randomly forced MHD turbulence with 256^3 grid points and periodic boundary conditions. The numerical method is described by Maron & Goldreich (2001). Both simulations use Newtonian viscosity and resistivity and are run until a statistical steady state is reached. In simulation A, there is no mean magnetic field and the initial conditions are a random-phase large-scale magnetic field with 10% of the maximum possible magnetic helicity. We include helicity because in its absence the magnetic spectrum becomes dominated by fluctuations on the resistive scale (Maron & Cowley 2001), which is not consistent with observed magnetic fields in clusters. In simulation C, there is a mean magnetic field $\langle \mathbf{B} \rangle$ comparable to the fluctuating magnetic field $\delta \mathbf{B}$, and the initial conditions include a random-phase large-scale magnetic perturbation ($\delta \mathbf{B} \sim \langle \mathbf{B} \rangle$) so that the initial field lines are chaotic. We also analyze field-line separation in numerically generated random-phase magnetic fields with Fourier amplitudes equal to those in simulations A and C. For both the numerically simulated fields and the random-phase fields, we determine $\langle l \rangle$ and $\langle l^2 \rangle$ by integrating the trajectories of 2000 field line pairs in each of four snapshots of the magnetic field separated in time by $0.2l_B/u$, where u is the rms turbulent velocity. We iteratively reduce the length step in the field-line integrations to achieve convergence. We remind the reader that $\langle l \rangle$ is the average distance in units of l_B that a field-line pair must be followed before separating by a distance l_B , and $\langle l^2 \rangle$ is the average of the square of the distance a field-line pair must be followed before separating by a distance l_B , expressed in units of l_B^2 . Results for $\langle l \rangle$ are shown in figure 3. We set π/l_B equal to the maximum of $kM(k)$, where $M(k)$ is the one-dimensional power spectrum of the magnetic field [the total magnetic energy is $\int M(k)dk$], and set π/l_d equal to the maximum of $k^3M(k)$. We evaluate characteristic values of a and b in the simulation by calculating the mean and mean-square increments to y for field-line pairs initially separated by a distance $l_B/8$ during a displacement of $l_B/4$ along the magnetic field. These same values of a , b , and l_B/l_d are used to obtain the Monte Carlo and analytic Fokker-Planck results in the of figure 3. Parameters for the simulations are given in table 2.

For the magnetic fields obtained in the direct numerical simulations, $\langle l \rangle$ is well fit by the formula

$$\langle l \rangle = m_1 + m_2 \ln(l_B/r_0) \quad (47)$$

for $l_d < r_0 \lesssim l_B$, with values of m_1 and m_2 given in table 2. If $\langle l \rangle$ were instead to asymptote to a constant value in the small- r_0/l_B limit for $r_0 > l_d$, we would see $\langle l \rangle$ fall below a purely logarithmic scaling for $r_0 = 0.05l_B - 0.2l_B$ in the simulation-A data, values of r_0 that are $\ll l_B$ and yet still in the inertial range. We

take the absence of any such trend as evidence that $\langle l \rangle$ continues to follow a logarithmic scaling for arbitrarily small r_0/l_B provided $r_0 > l_d$. On the other hand, for the random-phase fields and the Monte-Carlo solutions, $\langle l \rangle$ grows less than logarithmically with decreasing r_0 for $l_d < r_0 \lesssim l_B$. We suspect that the random-phase data, like the Fokker-Planck and Monte-Carlo results, would asymptote to a constant value in the small- r_0/l_B and small- l_d/l_B limits provided r_0 was not much smaller than l_d .

Our Fokker-Planck and Monte-Carlo models, like the earlier theoretical treatments discussed in the introduction, are reasonable models for the random-phase fields, but not for the structured turbulence in the numerical simulations. The most likely explanation is intermittency. The magnetic shear in the direct numerical simulations is concentrated into smaller regions than in the random-phase data; likewise, a large fraction of the volume has a relatively small amount of magnetic shear (“anti-intermittency”). The highest-shear regions are sheet-like with widths $\sim l_d$ and lengths $\sim l_B$ along the field (Maron & Goldreich 2001). These sheets are aligned with the magnetic field because the Alfvénic structures comprising the sheets propagate along the field. As a result, field lines outside of intermittent structures can be followed for long distances before they enter high-shear regions. The fraction of the volume filled by eddies or sheets of width λ_\perp may decrease with decreasing λ_\perp (Maron & Goldreich 2001). If this is the case, as r_0 is decreased, a field-line pair can be followed for a longer distance before it encounters the eddies or sheets of width r that are most effective at causing the field-line pair to separate. These effects limit the ability of small-scale fields to separate the majority of the closely-spaced field-line pairs. Although small-scale contribute significantly to field-line separation, the fluctuations at scale l_B are volume-filling and cause enough field-line separation on their own to give a result like equation (47) (Chandran & Cowley 1998).

The presence of a mean magnetic field in the simulations acts to inhibit field-line separation, presumably because there is more reversibility in field-line displacements perpendicular to the mean field. We note that for $r_0 = l_B$, $\langle l \rangle$ is by definition 0. The first solid circles in the left-hand panels correspond to $r_0 = 0.99l_B$, indicating that $\langle l \rangle$ is discontinuous at $r_0 = l_B$ in the numerical simulations. The reason is that for r_0 just slightly less than l_B , some fraction of the field line pairs are initially converging towards each other and must be followed a significant distance before they start to diverge. A subtlety for calculating $\langle l \rangle$ and $\langle l^2 \rangle / \langle l \rangle$ in simulation C is that a small fraction of the field-line pairs traverse the periodic simulation domain and end up close to the points at which they entered the simulation domain. Such field lines continue to follow nearly the same trajectories for many passages of the simulation domain, traveling extremely far before separating by a distance l_B . This small fraction of the field lines would make a considerable and spurious contribution to $\langle l \rangle$ and $\langle l^2 \rangle$. We thus reject such field-line pairs from the sample using criteria described in the companion paper Maron et al (2003).

We have focused on $\langle l \rangle$ because there is less scatter in the data than for $\langle l^2 \rangle / \langle l \rangle$. The data for $\langle l^2 \rangle / \langle l \rangle$, which is presented in the companion paper Maron et al (2003), is well fit by the formula

$$\frac{L_S}{l_B} = \frac{\langle l^2 \rangle}{\langle l \rangle} = c_1 + c_2 \ln(l_B/r_0) \quad (48)$$

for $l_d < r_0 < l_B$, with values of c_1 and c_2 given in table 2. This

scaling is approximately valid for r_0 as small as $l_d/40$, the value needed to calculate $L_S(\rho_e)$. ($\langle l^2 \rangle / \langle l \rangle > \langle l \rangle$ from the Schwartz inequality.)

To investigate the role of initial conditions on the values of $\langle l \rangle$ and L_S , we take random-phase versions of the developed turbulence in simulations A and C and use these random-phase fields as initial conditions in new simulations. After we run these new simulations for a moderate fraction of the large-eddy turnover time l_B/u , we find that the values of $\langle l \rangle$ and L_S return to the values obtained in the original simulations A and C. Thus, even from a highly-scrambled initial magnetic field, the turbulence evolves to a state in which $\langle l \rangle$ and L_S depend logarithmically on r_0 in the small- r_0/l_B limit.

In figure 4 we plot the probability distribution of the distance in units of l_B that a field line pair must be followed before it separates by a distance l_B . We define the function $\text{PDF}(l)$ so that the probability that l lies in some interval in one of the simulations is proportional to the corresponding area under the plotted curve for that simulation. For the simulation-A plot we take $r_0 = 3.8 \times 10^{-3} l_B$; for the simulation-C plot we take $r_0 = 1.2 \times 10^{-2} l_B$.

6. NUMERICAL EXAMPLE OF SUPPRESSION OF κ_T IN THE STATIC-FIELD APPROXIMATION

We consider 3C 295 at a distance of 100 kpc from cluster center with deprojected density $n_e = 0.01 \text{ cm}^{-3}$ and temperature $k_B T = 5 \text{ keV}$ (Allen et al 2001). Perley & Taylor (1991) estimated $l_B = 3.4 \text{ kpc}$ in 3C 295 from rotation-measure variations in the plane of the sky. From the dispersion in the rotation measure and the electron density profile in 3C 295, Allen et al (2001) found the intracluster magnetic field strength to be $12 \mu\text{G}$, assuming $l_B = 3.4 \text{ kpc}$. These parameters yield $\rho_e = 1.4 \times 10^7 \text{ cm}$, and $L_S(r_0) \simeq l_B [1.8 + 1.3 \ln(l_B/r_0)] = 46 l_B$ for $r_0 = \rho_e$. The static-field approximation then gives $\kappa_T \sim \kappa_S/46$.

7. THE EFFECTS OF EFFICIENT TURBULENT RESISTIVITY AND FIELD-LINE MIXING ON κ_T

In this section, we first estimate the consequences of the assumption that turbulent resistivity completely reconnects the magnetic field on the eddy turnover time τ at scale l_B , $\tau = l_B/u$, where u is the rms velocity and the velocity outer scale l_0 is assumed equal to l_B . A similar assumption was explored by Gruzinov (2002). We take $\tau > \lambda/v_{th}$ and $\lambda < L_S$, as appropriate for intracluster plasmas, where v_{th} is the electron thermal velocity and λ is the Coulomb mean free path. For typical cluster parameters, $\tau < (L_S^2/D_{||})$, and particles escape field lines primarily by field-line randomization. The fundamental random-walk step is of duration τ , during which a particle moves an rms distance $\sim \sqrt{D_{||}\tau}$ along the field and undergoes a three dimensional rms displacement $\sim [l_B \sqrt{D_{||}\tau}]^{1/2}$. The diffusion coefficient is then

$$D \sim \sqrt{D_{||} l_B}. \quad (49)$$

[If $\tau > L_S^2/D_{||}$, a particle escapes its initial field line primarily through parallel motion and $D \sim D_{||} l_B/L_S$ as in the static-field case. If $\tau < l_B^2/D_{||}$, i.e. $u l_B > D_{||}$, then the fundamental random walk step during a time τ is of length l_B , successive steps are uncorrelated because of the assumption of complete field randomization, and $D \sim u l_B$.] Equations (1), (13), and (49) imply

that

$$\frac{\kappa_T}{\kappa_S} \sim \sqrt{\frac{u l_B}{D_0}} \quad (50)$$

for $\tau < L_S^2/D_{||}$. To estimate the right-hand side of equation (50), we evaluate D_0 at a slightly superthermal value of v such that $D_0 = \kappa_S$, which gives

$$\kappa_T \sim \sqrt{\kappa_S u l_B}. \quad (51)$$

Field-line mixing may have a similar effect on κ_T even if field lines are not completely reconnected after a time l_B/u . For the purpose of this discussion, we continue to assume $l_0 = l_B$. If all the field lines within a box of volume l_B^3 are interchanged during a time l_B/u , then because of slow cross-field motions, an electron that starts on some field line F1 will, after a time l_B/u , find itself on a field F2 line that was initially a distance $\sim l_B$ away from F1. As the particle follows F2, it rapidly loses correlation with F1, even when $L_S(\rho_e)/l_B$ is very large. The maximum duration of the fundamental random-walk step of particle motion is then roughly l_B/u , and the resulting value of D is the same as if field lines are completely reconnected after a time l_B/u . There are two related problems with this scenario. First, it is possible that field-line mixing completely mixes field lines in a time l_B/u only within bundles of field lines that are coherent over long distances, or near intermittent regions of intense shear. Second, unless field lines are largely reconnected in a time l_B/u , they can not be completely interchanged if the field is initially tangled, and the efficiency of turbulent reconnection is not understood.

We emphasize that the results of this section are conjectural. Further work on turbulent resistivity, reconnection, and mixing is needed to clarify the roles of these processes in heat conduction.

8. SUMMARY

In this paper we consider the effects of field-line tangling, turbulent resistivity, and field-line mixing on the thermal conductivity κ_T in galaxy clusters. In the static-magnetic-field approximation, tangled field lines force electrons to move greater distances in traveling from hotter regions to colder regions, reducing κ_T by a factor of ~ 46 relative to the Spitzer thermal conductivity κ_S for typical cluster parameters. In the static-field approximation, heat conduction is too small to balance radiative cooling in clusters. It is possible that turbulent resistivity and field-line mixing enhance κ_T , but further work is required to investigate this possibility.

We thank Eric Blackman, Steve Cowley, and Alex Schekochihin for valuable discussions. This work was supported by NSF grant AST-0098086 and DOE grants DE-FG02-01ER54658 and DE-FC02-01ER54651 at the University of Iowa, with computing resources provided by the National Partnership for Advanced Computational Infrastructure and the National Center for Supercomputing Applications.

Allen, S., Taylor, G., Nulsen, P., Johnstone, R., David, L., Ettori, S., Fabian, A., Forman, W., Jones, C., & McNamara, B. 2001, *MNRAS*, 324, 842

Binney, J., & Cowie, L. 1981, *ApJ*, 247, 464

Binney, J., & Tabor, G. 1995, *MNRAS*, 276, 663

Bohringer, H., & Morfill, G. E. 1988, *ApJ*, 330, 609

Bregman, J., & David, L. 1989, *ApJ*, 341, 49

Chandran, B. 1997, *ApJ*, 485, 148

Chandran, B., & Cowley, S. 1998, *Phys. Rev. Lett.*, 80, 3077

- Chandran, B., & Rodriguez, O. 1997, *ApJ*, 490, 156
- Chandrasekhar, S. 1943, *Rev. Mod. Phys.*, 15, 1
- Cho, J., & Lazarian, A., 2003 *Phys. Rev. Lett.* in press
- Cho, J., & Vishniac, E. 2000, *ApJ*, 539, 273
- Chun, E., & Rosner, R. 1993, *ApJ*, 408
- Ciotti, L., & Ostriker, J. 2001, *ApJ*, 551, 131
- Churazov, E., Sunyaev, R., Forman, W., & Bohringer, H. 2002, *MNRAS*, 332, 729
- Crawford, C., Allen, S., Ebeling, H., Edge, A., Fabian, A. 1999, *MNRAS*, 306, 875
- Fabian, A. C. 1994, *Ann. Rev. Astr. Astrophys.*, 32, 277
- Fabian, A. C. 2002, *astro-ph/0210150*
- Goldreich, P. & Sridhar, S. 1995, *ApJ*, 438, 763
- Gruzinov, A. 2002, *astro-ph/0203031*
- Krommes, J., Oberman, C., & Kleva, R. 1983, *J. Plasma Phys.*, 30, 11
- Jokipii, J. 1973, *ApJ*, 183, 1029
- Lithwick, Y., & Goldreich, P. 2001, *ApJ*, 562, 279
- Malyshkin, L., & Kulsrud, R. 2001, *ApJ*, 549, 402
- Maron, J., Chandran, B., & Blackman, E. 2003, in preparation
- Maron, J., & Cowley, S. 2001, *astro-ph/0111008*
- Maron, J., & Goldreich, P. 2001, *ApJ*, 554, 1175
- Narayan, R., & Medvedev, M. 2001, *ApJ*, 562, 129
- Pedlar, A., Ghataure, H. S., Davies, R. C., Harrison, B. A., Perley, R., Crane, P. C., & Unger, S. W. 1990, *MNRAS*, 246, 477
- Perley, R., Taylor, G. 1991, *AJ*, 101, 1623
- Peterson, J. A. et al 2001, *A&A*, 365, L104
- Pistinner, S., & Eichler, D. 1998, *MNRAS*, 301, 49
- Quataert, E. 1998, *ApJ*, 500, 978
- Rechester, R., & Rosenbluth, M. 1978, *Phys. Rev. Lett.*, 40, 38
- Rosner, R., & Tucker, W. 1989, *ApJ*, 338, 761
- Skilling, J., McIvor, I., & Holmes, J. 1974, *MNRAS*, 167, 87P
- Tabor, G., & Binney, J. 1993, *MNRAS*, 263, 323
- Tamura, T. et al 2001, *A&A*, 365, L87
- Tao, L. 1995, *MNRAS*, 275, 965
- Taylor, G., Fabian, A., Allen, S. 2002, *MNRAS*, 334, 769
- Taylor, G., Govoni, F., Allen, S., Fabian, A. 2001, *MNRAS*, 326, 2
- Tribble, P. 1989, *MNRAS*, 238, 1247
- Tucker, W. H., & Rosner, R. 1983, *ApJ*, 267, 547
- Voigt, L. M., Schmidt, R. W., Fabian, A. C., Allen, S. W., & Johnstone, R. M. 2002, *Mon. Not. R. Astr. Soc.*, submitted (*astro-ph/0203312*)
- Zakamska, N., & Narayan, R. 2003, *ApJ*, in press

Notation	Meaning
l_B	dominant length scale of the magnetic field
l_d	magnetic dissipation scale
$\langle l \rangle$	average distance in units of l_B that a field-line pair must be followed before separating by a distance l_B
$\langle l^2 \rangle$	average square of the distance in units of l_B^2 that a field-line pair must be followed before separating by a distance l_B
$L_s(r_0)$	$l_B \langle l^2 \rangle / \langle l \rangle$ —characteristic distance a field-line pair separated by a distance r_0 must be followed before separating to l_B
ρ_e	electron gyroradius
κ_T	thermal conductivity
κ_S	Spitzer thermal conductivity in a non-magnetized plasma
D	3D single-electron diffusion coefficient
D_0	3D single-electron diffusion coefficient in a non-magnetized plasma
D_{\parallel}	diffusion coefficient for electron motion along the magnetic field
λ	thermal-electron Coulomb mean free path
u	rms turbulent velocity

TABLE 1
DEFINITIONS.

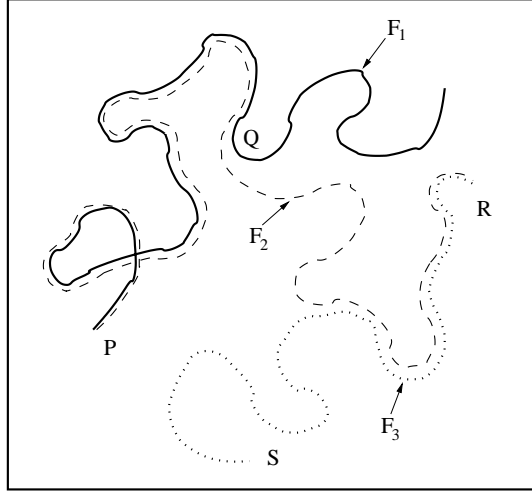


FIG. 1.— The solid line, dashed line, and dotted line represent three magnetic field lines, F_1 , F_2 , and F_3 . As explained in the text, a particle starting at point P on F_1 escapes F_1 through cross-field drifts and follows a new nearby field line F_2 which diverges from F_1 . The particle proceeds to point R, and then its collisional random walk along the magnetic field reverses direction. Instead of returning to point P, it again drifts across the field and follows a new field line to point S, undergoing a Markovian random walk and escaping the double-diffusion constraint of equation (7). The fundamental random-walk step involves moving a distance $\sim L_S$ along the magnetic field, where L_S is a characteristic distance that a particle must travel before it separates from its initial field line by a distance l_B (i.e., approximately the distance along the field from point P to point Q), and l_B is the dominant field length scale.

Simulation	Resolution	$\frac{\delta B}{ \langle \mathbf{B} \rangle }$	H_m	l_B/l_d	α	a	b	m_1	m_2	c_1	c_2
A	256^3	∞	0.1	33	1.2	0.31	0.22	0.7	1.0	1.8	1.3
C	256^3	1	0	11	0.16	0.13	0.085	1.5	4.0	8.5	5.5

TABLE 2

$\delta B/|\langle \mathbf{B} \rangle|$ IS THE RATIO OF THE RMS FLUCTUATING FIELD TO THE MEAN FIELD, H_m IS THE MAGNETIC HELICITY DIVIDED BY THE MAXIMUM POSSIBLE MAGNETIC HELICITY AT THAT LEVEL OF MAGNETIC ENERGY, α IS THE COEFFICIENT IN EQUATION (5), l_B/l_d IS THE RATIO OF OUTER SCALE TO INNER (DISSIPATION) SCALE, a AND b ARE CONSTANTS DESCRIBING THE RATE OF FIELD-LINE SEPARATION DEFINED IN EQUATIONS (18) AND (19), m_1 AND m_2 ARE FITTING PARAMETERS FOR $\langle l \rangle$ DEFINED IN EQUATION (47), AND c_1 AND c_2 ARE FITTING PARAMETERS FOR L_S DEFINED IN EQUATION (48).

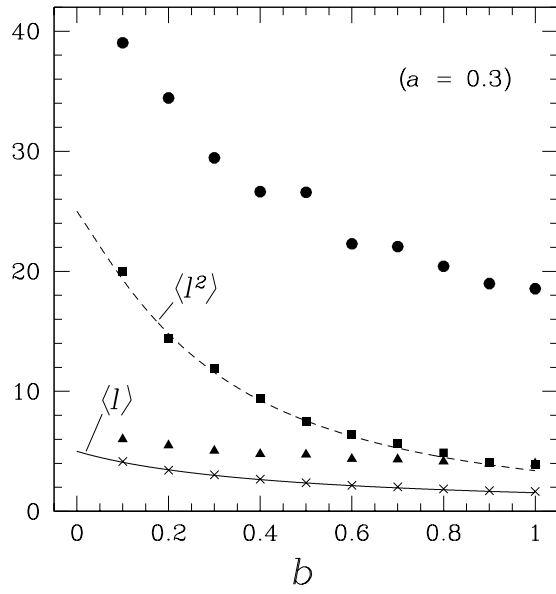


FIG. 2.— The solid line gives $\langle l \rangle$ from equation (44). The dashed line gives $\langle l^2 \rangle$ from equation (45). The \times s and squares give the values of $\langle l \rangle$ and $\langle l^2 \rangle$ from Monte Carlo calculations with $\phi = 10^{-4}$. The triangles and circles give the values of $\langle l \rangle$ and $\langle l^2 \rangle$ from Monte Carlo calculations with $\phi = 1$. For all data in plot, $a = 0.3$.

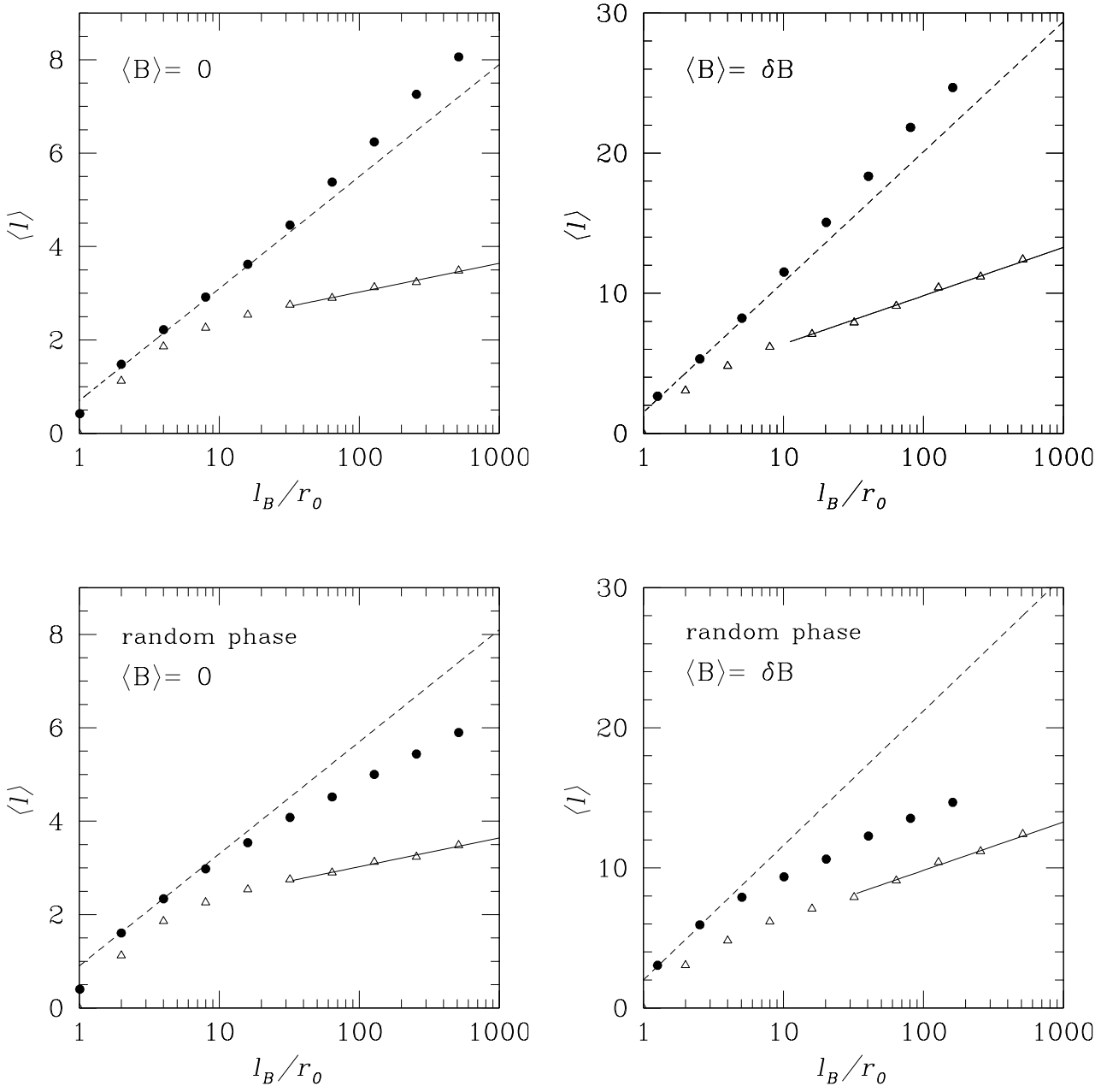


FIG. 3.— The solid circles correspond to simulation A (upper-left panel), simulation C (upper-right panel), a random-phase field with the same Fourier amplitudes as simulation A (lower-left), and a random-phase field with the same Fourier amplitudes as simulation C (lower-right). Dashed lines are straight lines added to aid the eye in determining whether the the solid circles are consistent with $\langle l \rangle$ being proportional to $\ln(l_B/r_0)$ for r_0 in the inertial range. Open triangles are Monte Carlo solutions with $\phi = 10^{-4}$, solid lines give the analytic Fokker-Planck solution [equation (43)]. The Monte Carlo and Fokker-Planck solutions in the two left-hand panels are identical, with $a = 0.31$, $b = 0.22$, and $l_B/l_d = 33$ (values corresponding to simulation A). The Monte Carlo and Fokker-Planck solutions in the two right-hand panels are identical, with $a = 0.13$, $b = 0.085$, and $l_B/l_d = 11$ (values corresponding to simulation C).

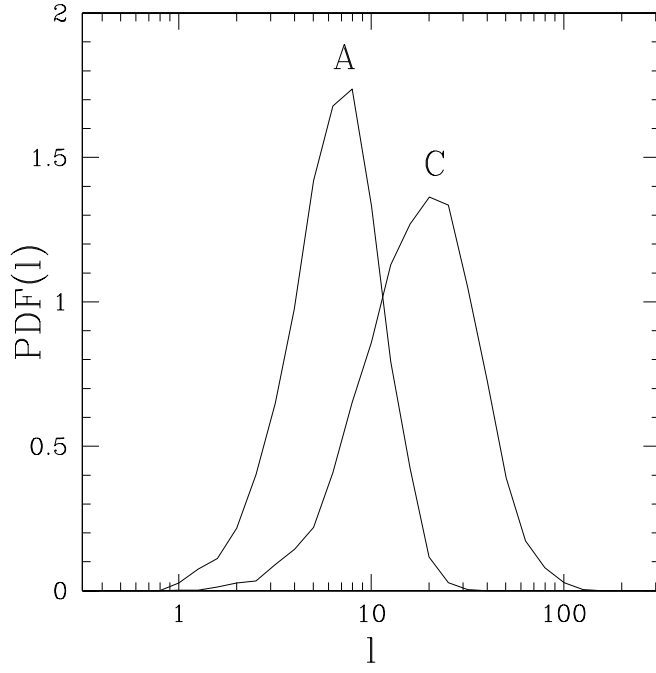


FIG. 4.— Probability distribution of the distance (in units of l_B) a field-line pair must be followed before separating by a distance l_B . For the simulation-A plot, $r_0 = 3.8 \times 10^{-3} l_B$; for the simulation-C plot, $r_0 = 1.2 \times 10^{-2} l_B$.